Journal of Statistical Physics, Vol. 116, Nos. 1/4, August 2004 (© 2004)

Planar Pyrochlore, Quantum Ice and Sliding Ice

R. Moessner,[1] Oleg Tchernyshyov,[2] and S. L. Sondhi[3]

Received August 1, 2003; accepted March 1, 2004

We study quantum antiferromagnetism on the highly frustrated planar pyrochlore lattice, also known as the square lattice with crossings. The quantum Heisenberg antiferromagnet on this lattice is of interest as a two-dimensional analogue of the pyrochlore lattice magnet. By combining several approaches we conclude that this system is most likely ordered for all values of spin, S, with a two-fold degenerate valence-bond solid being the ground state for small S. We show next that the Ising antiferromagnet with a weak four-spin exchange, equivalent to square ice with the leading quantum dynamics, exhibits analogous plaquette order. As a byproduct of this analysis we obtain, in the system of weakly coupled ice planes, a sliding phase with XY symmetry; at intermediate couplings, long range "anti-ferroelectric" order is stabilized.

KEY WORDS: Frustration; ice; sliding phase; quantum magnetism.

1. INTRODUCTION

On the heels of recent progress in understanding highly frustrated classical magnets, coupled with a substantial experimental effort,[(1)] renewed attention is now focused on the behavior of their quantum counterparts. In particular, the Heisenberg pyrochlore antiferromagnet is being studied with view to the question of whether frustration-enhanced quantum fluctuations might lead to unconventional ordering—or complete absence thereof—especially for small values of the quantum spin, S.[(2–8)] This model classically is special in that frustration prevents any sort of ordering or dynamical

[1] Laboratoire de Physique Théorique, École Normale Supérieure, CNRS-UMR 8549, Paris, France.

[2] Department of Physics and Astronomy, Johns Hopkins University, Baltimore, Maryland 21218.

[3] Department of Physics, Princeton University, Princeton, New Jersey 08544; e-mail: sondhi@princeton.edu

0022-4715/04/0800-0755/0 © 2004 Plenum Publishing Corporation

phase transition down to the lowest temperatures,[9–11] for which reason it is termed a cooperative paramagnet or classical spin liquid.

The challenge of this problem arises from the small energy scale generated by the frustration: in a semiclassical picture, any linear combination of the classically degenerate ground states—the collection of which is of extensive dimensionality[11]—may be selected as the quantum ground state. For the highly frustrated two-dimensional magnet on the related kagome lattice,[12] exact diagonalizations of small clusters[13] have provided crucial benchmarks. This system has turned out to be particularly well suited to this approach as it appears to have a very short correlation length, although one does find a large number of low-lying singlet excitations.

For the pyrochlore magnet, it looks as if such results will elude us for some time to come. The pyrochlore lattice, being three-dimensional, displays a more inclement scaling of the Hilbert space dimension with linear system size. Moreover, its unit cell contains four spins and its structure implies that the smallest system without spurious boundary condition effects contains at the very least 16 sites.

To evade this, attention has shifted to a system which avoids some of these complications, namely the planar pyrochlore lattice (Fig. 1). We note that the planar pyrochlore lattice, up to a mapping, has a prominent place in the history of exactly solvable two-dimensional models: the ground states of an Ising antiferromagnet map onto the states of square ice, the entropy of which was determined by Lieb in 1967.[14] We dedicate this paper to Elliott Lieb on the occasion of his 70th birthday.

The Heisenberg magnet on the planar pyrochlore lattice is expected to have similar properties to the pyrochlore as it has the same local structure—both can be thought of as networks of corner-sharing tetrahedra. Further, the size and topology of its ground state manifold for Heisenberg magnets are identical to the pyrochlore case.[11] However, it has a unit cell

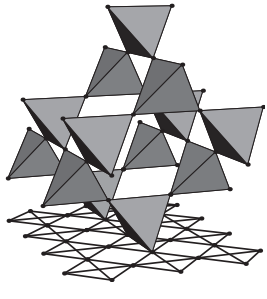

Fig. 1. The planar pyrochlore lattice, which can be obtained by projecting the 3-d pyrchlore lattice onto two dimensions. The spins reside on the underlying square lattice; a tetrahedron becomes a square with crossings upon projection, all bonds of which have equal strength.

of only two spins, is two dimensional, and has allowed exact diagonalizations of a good number of finite size systems of up to 36 spins. Such diagonalizations have been carried out by Palmer and Chalker[15] and by Fouet *et al.*[16] and other workers have also studied this system by several techniques.[8, 17–20]

In this paper, we take a somewhat broader view of quantum antiferromagnetism on the planar pyrochlore lattice. For the Heisenberg problem, apart from the small S cases, which we study by a dimer model analysis and a bosonic Sp(N) theory, we analyze the large S region, both within Sp(N)—which is also able to treat the intermediate region—and through the semiclassical $1/S$ expansion. Overall, we find a strong ordering tendency. In particular, there is a two-fold degenerate valence bond crystal for $S = 1/2$ (see Fig. 2). At large S the Sp(N) theory predicts a Néel phase, whereas the $1/S$ expansion finds a residual discrete degeneracy. Our predictions find support in the numerical work of Fouet *et al.* as we discuss further below. The nature of the valence bond order is at odds with other recent work.[8] The $S = 1/2$ kagome magnet[13] behaves very differently from the planar pyrochlore lattice—and therefore probably the pyrochlore —ones. Details of the ordering, however, depend on properties of the planar pyrochlore lattice (most prominently, the explicit breaking of the symmetry between bonds in a tetrahedron and the existence of nontrivial closed loops of length four residing on a bipartite lattice) which it does not share with the pyrochlore lattice; there we expect the order to be much more delicate.

In addition we consider the Ising antiferromagnet with a weak four spin exchange dynamics—the Ising ground states are isomorphic to those of square ice and the dynamics represent the shortest ring exchanges in this manifold arising from quantum tunneling—hence "quantum ice." The

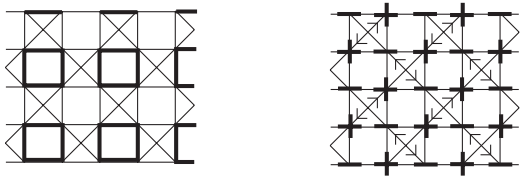

Fig. 2. Phases of magnets on the planar pyrochlore lattice discussed in this paper: the plaquette (left) and Néel (antiferroelectric) phases. The former describes the Heisenberg magnet at small S, in which case fat bonds are those with enhanced probability of singlet formation. It also describes the Ising magnet with weak ring exchange ("quantum ice"), in which context the enclosed fat plaquettes are those with a high expectation value of the resonance energy. The latter applies to ferromagnetically stacked Ising planes at intermediate coupling.

resulting state displays plaquette order analogous to the Heisenberg magnet at small S; this ordering agrees with results from exact diagonalizations.[21]

A byproduct of this analysis is the state of a stack of weakly coupled ice layers, which is seen to be in a "sliding" phase of the kind discussed in recent work,[22] albeit one that is protected by much simpler arrangements. At intermediate coupling, this sliding phase terminates in long range "antiferroelectric" order in ice terminology, or Néel order in Ising terminology (Fig. 2).

We turn now to the details of these assertions and sketches of the underlying analyses. We treat the Heisenberg problem first, for which the Hamiltonian is given by

$$H = J \sum_{\langle ij \rangle} \mathbf{S}_i \cdot \mathbf{S}_j, \tag{1.1}$$

where $J > 0$, the sum runs over all the bonds and the $\mathbf{S}$ are spin operators.

2. Sp(N) GENERALIZATION

The Sp(N) technology for frustrated magnets, a reformulation of Schwinger boson mean field theory[23] controlled by the introduction of $1/N$ as a small parameter, was introduced and described in detail by Read and Sachdev.[24] One starts by rewriting the SU(2) $\sim$ Sp(1) spin operators in terms of bosonic operators, $\{b_\uparrow, b_\downarrow\}$, with the constraint of $b_\uparrow^\dagger b_\uparrow + b_\downarrow^\dagger b_\downarrow = 2S$ on each site, and $S^z = (b_\uparrow^\dagger b_\uparrow - b_\downarrow^\dagger b_\downarrow)/2$, $S^+ = b_\uparrow^\dagger b_\downarrow$. The antiferromagnetic nearest-neighbor Heisenberg Hamiltonian is rewritten in terms of the bosonic operators:

$$H = -J \sum_{\langle ij \rangle} \{(\epsilon^{\sigma\tau} b_{i\sigma}^\dagger b_{j\tau}^\dagger/\sqrt{2})(\epsilon^{\mu\nu} b_{i\mu} b_{j\nu}/\sqrt{2}) - 1/4\}. \tag{2.1}$$

One generalizes this expression to Sp(N) by formally introducing N flavors of bosons, labeled by capital letters, and replacing the antisymmetric tensor in H by its Sp(N) generalization $\mathcal{J}_{AB}^{\mu\nu} = \epsilon^{\mu\nu}\delta_{AB}$. In the limit $N \to \infty$ at a fixed boson number per flavor per site, κ, one obtains to leading order in $1/N$ a mean-field theory for spin $S = \kappa/2$; fluctuations about this give rise to a gauge theory.

Self-consistent solutions to the mean field theory are obtained by minimizing with respect to the Hubbard–Stratonovich link fields $Q_{ij} = \langle \mathcal{J}_{AB}^{\mu\nu} b_{i\mu}^A b_{j\nu}^B \rangle$, subject to a constraint on the boson number κ. In the process, one obtains a dispersion relation for the energies ω of bosonic spin 1/2 quasiparticles. Within the mean-field theory, there is generically a disordered phase at small κ; when one of the bosonic modes goes soft as κ is

increased, condensation of these "spinons" occurs, and long-range spin order ensues.

Our results at mean-field level are readily summarized. We find zero expectation value of the diagonal bond variables at all κ. On the remaining bonds, long-range Néel order (Fig. 2) develops above $\kappa_c = 0.393$, exactly as for the simple square lattice. For $\kappa < \kappa_c$, the Néel correlations are only short-ranged.

Whether or not the spinon excitations in the disordered, small κ phase remain deconfined can only be settled by going beyond mean-field theory. As on the square lattice, one obtains a compact $U(1)$ gauge theory at $O(1/N)$, in which instanton tunneling effects lead to the formation of bond (Peierls) order.[24] An analogous calculation is presented by Chung *et al.* for the Shastry–Sutherland model.[25] Details of the ordering pattern, in particular those due to the inequivalence of the plaquettes with and without crossings, are perhaps most easily studied through a quantum dimer model (QDM), which we study for the case of SU(2) spins in the following section.

3. QUANTUM DIMER MODEL

This approach starts from the assumption that the magnet is in a regime where the Néel state is destabilized and the effective degrees of freedom are singlet bonds between neighboring spins, also called valence bonds, which are represented by dimers. As each spin participates in exactly one singlet bond, the Hilbert space consists of all hardcore dimer coverings. An effective dimer Hamiltonian is obtained by means of an overlap expansion, described in ref. 26. It is formally perturbative in a small parameter, x, arising from the non-orthogonality of the spin wavefunctions describing the different dimer coverings. When superimposing two dimer coverings, one obtains a set of closed loops, and each such loop contributes a factor of $x^{L/2-1}$ to the overlap, where L is the length of the loop (i.e., the loop is made up of $L/2$ dimers of each configuration). For $S = 1/2$ Heisenberg SU(2) spins, one finds $x = 1/2$.

To zeroth order in x, all of the exponentially numerous dimer coverings are degenerate. With the overlap expansion organized by length, L, of the resonance loops, the leading order quantum dynamics is a resonance process on the shortest possible resonance loop. In the case of the planar pyrochlore lattice, this has length four, and corresponds to flipping a pair of dimers by 90° (Fig. 3):  $\leftrightarrow$  , yielding the following Hamiltonian (see Appendix A):

$$H_{\mathrm{QDM}} = -\sum t_\alpha \hat{T}_\alpha = -\sum_{\square} t_\alpha (|\ \rangle\langle\ | + h.c.), \tag{3.1}$$

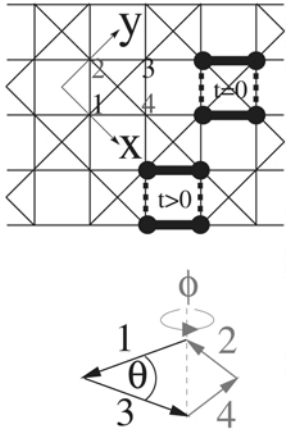

Fig. 3. Top: Numbers label the sublattices of the four-sublattice state. Numbers 1 and 2 in addition label sublattices used in the Monte Carlo simulation, and the arrows denote the translation vectors of the square lattice with basis making up the planar pyrochlore lattice. The two inequivalent resonance moves of the QDM are depicted. The one around the crossed plaquette has zero kinetic energy, $t_c = 0$. Bottom: Parametrization of the four-sublattice ground states on the planar pyrochlore lattice. For the Néel state, $\theta = \pi$ (and ϕ is arbitrary): $\mathbf{S}_1 = -\mathbf{S}_2 = \mathbf{S}_3 = -\mathbf{S}_4$. Spins 1 and 4 lie in the plane, spins 2 and 3 do not for $\phi \neq 0, \pi$.

where the sum is over all plaquettes, with the kinetic (resonance) energy t_α depending on whether the plaquette, $\square$, is crossed (t_c) or not (t_u). For the Rokhsar–Kivelson quantum dimer model, one obtains $t_c = 0$ and $t_u > 0$ (see Appendix A).

The vanishing of t_c arises because the equal amplitude superposition of two dimer states with the appropriate sign yields a third, degenerate dimer state of the plaquette. Put otherwise, the resonance move depicted in Fig. 3 induces diagonal triplet correlations which exactly cancel out the gain in resonance energy for the plaquettes with diagonal antiferromagnetic bonds. Note that *uncrossed* loops of length four are absent from the pyrochlore lattice, where the shortest loop contacting more than one tetrahedron has length six. The question is what kind of quantum dimer state is selected by this resonance move.

Extending the results from the square lattice QDM,[26] one therefore expects the resulting state to be a valence bond crystal; the staggering of t strongly favors the plaquette crystal, with the dimers resonating on one of two sublattices of plaquettes without crossings (Fig. 2). This is because a columnar valence bond crystal would reduce the resonance energy gained from the uncrossed plaquettes without an offsetting gain from the crossed ones.

Note that the degeneracy of this state is two rather than four, as would be the case for the plaquette state on the square lattice, because of the explicit symmetry breaking introduced by the presence of the plaquettes with crossing interactions.

4. SEMICLASSICS

We now consider the case of large spin S and large κ for SU(2) and Sp(N), respectively. To see which state is favored by quantum fluctuations at leading order in $1/S$ and $1/N$, one compares the zero-point energy, $\sum_\kappa \hbar\omega_\kappa/2$ of the bosonic excitations (spin waves and spinons, respectively, with frequency ω_κ) of different, classically degenerate ground states. This, in principle, requires evaluating that energy for the entire ground state manifold, which is of extensive dimensionality.

For Sp(N), we have compared the bosonic zero-point energies[24] of all four-sublattice states (see Fig. 4), as well as of eight-sublattice coplanar states. The four-sublattice states are those states which consist of a single-tetrahedron ground-state repeated identically on one of the two sublattices of tetrahedra. These states can be parametrized by two angles θ and ϕ, as depicted in Fig. 3. Similarly, the eight-sublattice states consist of identical repetitions of eight spins on two tetrahedra. We find that the Néel state selected at κ_c is also favored in this limit, which suggests its stability for all $\kappa > \kappa_c$.

For large S, we have computed the zero-point energy of all four-sublattice states (see Fig. 4). This turns out to be most conveniently done using the equations of motion for the total magnetizations of the tetrahedra, which were derived in ref. 11. For a given wavevector, the mode energies are given by an antisymmetric traceless 3×3 matrix, which implies that all such states have a zero-energy branch in their excitation spectrum in addition to the "standard" zero energy branch present for all ground states.[11] Note that these zero point energies do not diverge despite the presence of the zero-frequency modes.

We find qualitative agreement with Henley's suggestion[27] of an effective energy functional of the biquadratic type, $-\sum_{\langle ij \rangle} (\mathbf{S}_i \cdot \mathbf{S}_j)^2$, in that it correctly reproduces the location of the maximum and the minima. There remains a degeneracy between some inequivalent collinear states.[27] One of the remaining degenerate states is indeed the Néel state, but other states, disfavored at $O(1/\kappa)$, still have exactly the same energy of zero-point fluctuations at $O(1/S)$. As discussed in a different context, the planar pyrochlore lattice Heisenberg model at leading order in $1/S$ does indeed retain a subextensive degeneracy.[27, 28] The fate of this degeneracy at higher order in $1/S$ remains unknown. We note that the large-κ treatment of

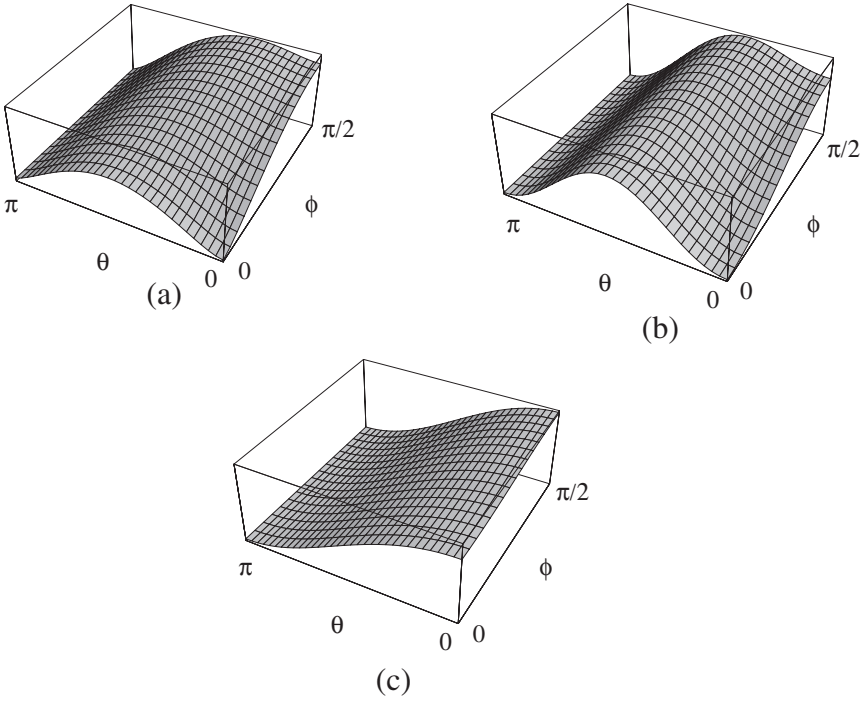

Fig. 4. Zero-point energy of four-sublattice states on the planar pyrochlore lattice as a function of θ and ϕ (see Fig. 3): (a) large-S Heisenberg; (b) biquadratic $-\sum_{\langle ij \rangle} (\mathbf{S}_i \cdot \mathbf{S}_j)^2$; (c) large-$\kappa$ for Sp(N). For ease of comparison, the scales of the energy (z-axis) have been chosen such that the difference of maximal and minimal energy are the same for all three plots. The energies are invariant under $\phi \to \pi \pm \phi$.

Sp(N) differs significantly from both the large-S expressions. We discuss the detailed origin of this effect elsewhere.[29]

5. IMPLICATIONS FOR THE 3-D PYROCHLORE MAGNET

The actual ordering behavior of the $S = 1/2$ pyrochlore magnet is still far from settled. At this stage[2–8, 27] it appears to be somewhat closer to that of the planar pyrochlore lattice than either of the two is to the kagome case, where there has so far been no strong indication of long-range order of any kind for $S = 1/2$, and where the large-S state is necessarily non-collinear. We emphasize, however, that details of the ordering we find, such as the pattern of the bond solid or the size of the unit cell, crucially depend on differences between the two lattices—such as spatial dimensionality, the presence of inequivalent links, and short closed loops linking different

tetrahedra. Moreover, we remark that most approaches employed so far for $d = 3$ pyrochlore[2–4, 6–8] explicitly remove the equivalence of all tetrahedra by weakening the bonds on half of them; from such a starting point, it would would seem rather difficult to restore this equivalence perturbatively, which is necessary for obtaining the plaquette ordering we find.

6. FINITE-SIZE DIAGONALIZATIONS

The agreement of the above calculations on a number of central points is reassuring. Most importantly, they are all consistent with ordered states with translational symmetry breaking and a two-fold degeneracy. For small S, they lead us to expect dimer order of the plaquette flavor. How does this compare to exact diagonalizations of $S = 1/2$ Heisenberg magnets?

Palmer and Chalker, who have studied systems containing up to 24 spins, find no clearly identifiable degeneracy. Rather, there appears to be a large number of low-lying singlet states with a small gap and a much larger gap to triplet excitations. They rule out Néel order but are inconclusive about translational symmetry breaking. Fouet *et al.* agree with their results, but have in addition studied a system with 36 sites. There, they find a particularly low ground state energy, suggesting that the boundary conditions for this system size accommodate well the quantum ground state.[30] For this system, there does appear a two-fold near degeneracy of the ground state, with the states being described by the wavevectors expected for our dimer crystal.

7. QUANTUM ICE

We turn next to the Ising problem, whose Hamiltonian is given in analogy to Eq. (1.1):

$$H = J \sum_{\langle ij \rangle} \sigma_i^z \sigma_j^z; \tag{7.1}$$

here, the σ are Pauli matrices. This by itself has no dynamics. In the following, we consider the simplest quantum dynamics in the ground state manifold. This is a "ring exchange" process in which four antiferromagnetically arranged spins around a square *without* crossings reverse orientation. In six vertex language this is a reversal of a closed loop of arrows. In the physical three dimensional ice problem, as a matter of principle, the degeneracy of the low energy manifold will be lifted by quantum effects which will involve exactly such processes in which a set of hydrogens move

coherently. Our two dimensional model mimics such processes, much as the square ice problem mimics real ice. The issue now is whether such a dynamics gives rise to ordering.

In the Ising spin representation on the planar pyrochlore lattice the dynamics is represented by the Hamiltonian, H_Q, acting between ground states of the classical model,

$$H_Q = -\Gamma \sum_p (\sigma^+\sigma^-\sigma^+\sigma^+ + \text{h.c.}) \tag{7.2}$$

where p denotes a sum over non-crossed plaquettes of the lattice, and $\sigma^{+(-)}$ are the raising(lowering) operators of the Ising spins $\sigma^z = \pm 1$. To study this Hamiltonian it is convenient to use an imaginary time discrete representation of the path integral via the standard Trotter–Suzuki procedure. Here, this procedure yields a $d = 2+1$ system consisting of a set of ferromagnetically stacked planes of the planar pyrochlore lattice:

$$H_C = K^\tau \sum_{i,n} \sigma^z_{i,n}\sigma^z_{i,n+1}, \tag{7.3}$$

where we have introduced an additional layer index n in the imaginary time direction and the restriction of the spatial planes to the ground states of Eq. (7.1) is implicit. The quantum dynamics is captured correctly in the time continuum limit at large ferromagnetic interlayer coupling, $K^\tau \to \infty$. For details of this mapping, see ref. 31, where it is discussed in the context of a study of the quantum dynamics of transverse field Ising models on a range of frustrated lattices.

We have carried out a Monte Carlo simulation on this stacked model, with the spin-flip of four spins around a non-crossed plaquette as the basic Monte Carlo move. We have utilized a cluster algorithm in the imaginary time direction, and restricted allowed world line configurations to those consistent with the quantum dynamics, that is to say that going from one layer to its neighbors, only spins on a single plaquette may be flipped together, and not larger compounds. In the limit $K^\tau \to \infty$, this restriction is enforced automatically by the energetics, but for small K^τ, two neighboring planes may differ, e.g., by only six spins on two adjacent plaquettes.

The results of this simulation are depicted in Fig. 5, where we have plotted the spin–spin correlations for spins on one sublattice along the coordinate axes as well as the "flippability" correlations, as defined in the figure caption. We find that the spin correlations rapdily and featurelessly decay to zero whereas there clearly is long-range order of the flippability at wavevector (π, π). This state is thus plaquette ordered as depicted in Fig. 2, where the plaquettes denoted by heavy lines have an enhanced resonance

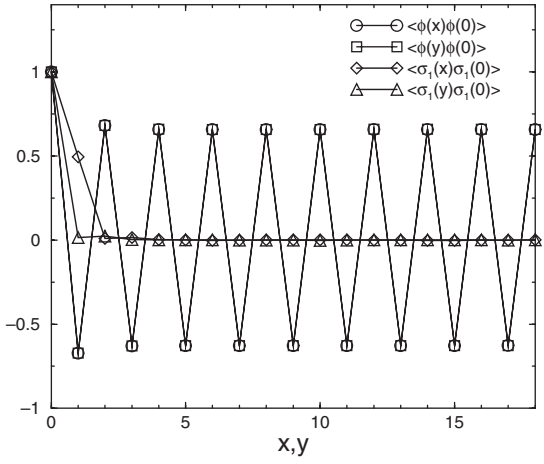

Fig. 5. Flippability, ϕ, and spin, σ_1, correlations from quantum Monte Carlo on $36 \times 36 \times 256$ plaquettes. The spin correlations refer to spins on sublattice one in a given timeslice. Similarly, the ϕ variables measure if a given uncrossed plaquette is flippable or not, $\phi = \pm 1$. The sublattices and directions are defined in Fig. 3.

energy. Such an ordered state has been found from exact diagonalizations, by Ph. Sindzingre, for the Heisenberg–Ising model on the planar pyrochlore lattice close to the Ising limit.[21]

Finally, we note that the quantum dynamics discussed here can perturbatively be induced by a ring exchange, a transverse exchange of either sign, or a transverse field.

8. SLIDING ICE

It turns out to be interesting to study the imaginary time representation Eq. (7.3) in the *weak* coupling limit, $K^\tau \ll 1$. While this is no longer equivalent to the starting quantum Hamiltonian (7.2), it can be interpreted as the classical statistical mechanics of a set of square ice planes with a potential interaction between the planes. In this limit the interaction competes with the entropy of the planes and we may ask if the entropy prevails and leads to a "sliding phase," such as those introduced recently in studies of stacked XY systems,[22] in which the individual layers continue to exhibit algebraic correlations. To answer this we appeal to the height representation description of the Ising ground state (ice) manifold, which we provide in the following.

The ground states of the Ising antiferromagnet on the planar pyrochlore lattice require two up and two down spins on each tetrahedron

(square with crossings). The six such possible configurations on each tetrahedron can be identified with the allowed vertices of the six-vertex model as follows.[32] Divide the square lattice consisting of the crossings at the centers of the tetrahedra into sublattices A and B in the usual fashion. Orient the links coming out of sublattice A(B) inwards if the spin sitting on that link is up(down) and outwards if the spin in down(up) (Fig. 2). As all vertices are weighted equally, the ground state manifold has the extensive entropy, $(3/4)\ln(4/3)$ per spin, of square ice.[14]

The ice problem also has a height representation in which an integer valued height living on the dual lattice steps up(down) by one on crossing an in(out) arrow clockwise around any vertex. By the standard logic for such representations, the coarse grained heights are are weighted by the pseudo-Boltzmann factor:[33]

$$\rho[h(\mathbf{x})] \propto e^{-\int d^2x[\frac{\pi}{12}(\nabla h)^2+\lambda\cos(2\pi h)]}, \tag{8.1}$$

where the second term keeps track of the discreteness of the microscopic heights. With the stiffness exhibited for the ice problem, this term is irrelevant.

In order to compute the spin correlations for the original Ising variables, we need to identify the most relevant long wavelength operators that arise in their expansion. As there are two spins per unit cell, two identifications are needed. Using the labeling for the unit cell and the lattice axes shown in Fig. 3, we find that the spins are represented by the operators,

$$\begin{aligned}\sigma_1 &\sim (-1)^{x+y}\,\partial_x h+\frac{v}{2i}(e^{i\pi h}-e^{-i\pi h})+\cdots\\ \sigma_2 &\sim -(-1)^{x+y+1}\,\partial_y h-\frac{v}{2i}(e^{i\pi h}-e^{-i\pi h})+\cdots.\end{aligned} \tag{8.2}$$

The choice of operators is restricted by the global periodicity of the microscopic height representation under $h\to h+2$, and the observation that $h\to h+1$ and $h\to -h$ interchange the two flat microscopic states, which are the two Néel states on the square lattice with the crossings removed. As a consequence, the vertex operator pieces—which are the first subleading terms—must enter oppositely in the expressions for σ_1 and σ_2 but the remaining sign choice is inconsequential. Our interest in keeping the subleading terms will become clear in the following.

From the above identifications we can deduce the asymptotics of the spin correlations. We find algebraic decay with two dominant wavevectors,

$$\begin{aligned}
\langle\sigma_1(0)\,\sigma_1(x,y)\rangle &\sim (-1)^{x+y}\,\Xi\,\frac{y^2-x^2}{(x^2+y^2)^2}+\frac{\Upsilon}{(x^2+y^2)^{3/2}}\\
\langle\sigma_2(0)\,\sigma_2(x,y)\rangle &\sim (-1)^{x+y}\,\Xi\,\frac{x^2-y^2}{(x^2+y^2)^2}+\frac{\Upsilon}{(x^2+y^2)^{3/2}}\\
\langle\sigma_1(0)\,\sigma_2(x,y)\rangle &\sim (-1)^{x+y}\,\Xi\,\frac{2xy}{(x^2+y^2)^2}-\frac{\Upsilon}{(x^2+y^2)^{3/2}}\\
\langle\sigma_2(0)\,\sigma_1(x,y)\rangle &= \langle\sigma_1(0)\,\sigma_2(x,y)\rangle
\end{aligned} \tag{8.3}$$

where $\Xi = 3/\pi^2$ and $\Upsilon = v^2/2$ with the vertex operators normalized to give power laws with unit coefficients. The (π,π) component was discussed extensively in ref. 34, and reflects the local conservation of polarization in the ice problem. Along the x axis, $\langle\sigma_1(0)\,\sigma_1(x,0)\rangle$, can be deduced,[34] from exact results on one dimensional quantum systems. This proceeds via the recognition that the Hamiltonian of the Heisenberg–Ising chain

$$H = -\sum_n S_n^x S_{n+1}^x + S_n^y S_{n+1}^y + \Delta S_n^z\, S_{n+1}^z \tag{8.4}$$

commutes with the transfer matrix of the six vertex problem along the y directions, whence its ground state is also the dominant eigenvector of the latter. The ice problem corresponds to $\Delta = 1/2$ and the first two pieces of Eq. (8.3) correspond to the uniform and staggered correlations of the spin chain. The roles are switched due to the extra staggering in going between the planar pyrochlore spins and the ice variables. Our full form, guessed from the height representation, is thus consistent with these known results. Recent work by Lukyanov on the asymptotics of spin correlations of the Heisenberg–Ising chain[35] has provided an analytic expression for the amplitude Υ. The expression is sufficiently complicated that we will content ourselves by noting that $\Upsilon = 0.01795\ldots$.

For uncoupled planes, the probability distribution

$$\rho[\{h_n(\mathbf{x})\}] \propto \prod_n e^{-\int d^2x[\frac{\pi}{12}(\nabla h_n)^2]}, \tag{8.5}$$

is a fixed point of a two-dimensional renormalization group (RG) transformation in the standard fashion. The coupling between the planes induces two perturbations in the height language: the first of these,

$$\phi_1 = \sum_n \int d^2x(\nabla h_n)\cdot(\nabla h_{n+1}), \tag{8.6}$$

is exactly marginal under the RG while the second

$$\phi_2 = \sum_n \int d^2x \sin[\pi h_n] \sin[\pi h_{n+1}] \tag{8.7}$$

is irrelevant as is readily verified. It follows then that the system exhibits a sliding phase at weak coupling, whence "sliding ice." One can also check that the effect of the marginal term is to make ϕ_2 less irrelevant, suggesting that it eventually locks the planes together.

We have carried out Monte Carlo simulations to test this, the results of which are depicted in Fig. 6. There, we plot the spin–spin correlations for spins on one sublattice as a function of distance in the x-direction (see Fig. 3 for the conventions used). For $K^\tau = 0$, we are in the classical limit (decoupled planes), and we have checked that our simulations reproduce the correct power law decay of the spin–spin correlation function there. We find that this phase remains stable at small ferromagnetic coupling—the curves for $K^\tau = 0$ and $K^\tau = 0.1$ are virtually indistinguishable, thus confirming the existence of the sliding phase.[36]

As K^τ is increased further, long-range spin order ensues, as evidenced by the non-zero long-range piece of the spin correlation function at $K^\tau = 0.2$. We have checked that the spins on the other sublattice order with an opposite sign. The heights therefore undergo a locking transition between $K^\tau = 0.1$ and $K^\tau = 0.2$.

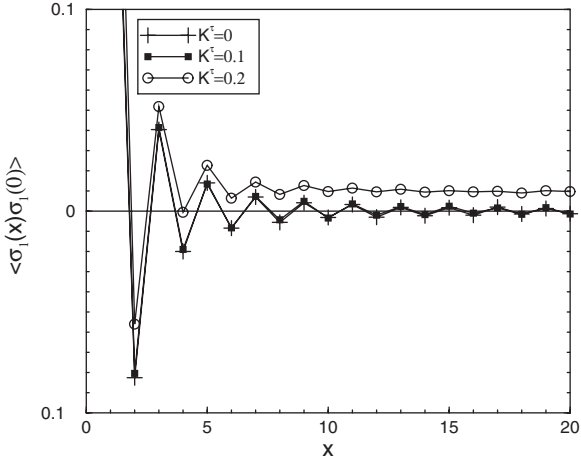

Fig. 6. Spin correlations on sublattice 1 in the x-direction from Monte Carlo on $48 \times 48 \times 16$ plaquettes. The classical curve, $K^\tau = 0$, and $K^\tau = 0.1$ coincide. Néel long-range order, albeit weak, obtains for $K^\tau = 0.2$.

For the spins on the planar pyrochlore lattice this is Néel order. Translated back into ice language, our results indicate that the system exhibits long range order of the antiferroelectric (or F model) kind (Fig. 2) at intermediate coupling, in which it maximizes the density of flippable plaquettes. We are currently investigating the details of the transition from the antiferroelectric to the plaquette state as K^{τ} is increased.

In height language, both the antiferroelectric and the plaquette ordered state correspond to a flat phase with heights in adjacent layers locked. While it is natural to expect that one gets a flat phase, the minimal information we have used to set up the height analysis does not allow us to decide analytically which flat state is actually realized. For determining this 'detail' of the ordering, the simulations were necessary. Irrespective of this, locked heights in the limit $K^{\tau} \to \infty$ imply a gap for quantum ice.

9. SLIDING XY CHAINS

As we have already noted earlier, there is an intimate connection between the six vertex problem and the XXZ chain. Our above discussion of the sliding ice phase can be lifted *mutatus mutandis* into an account of a sliding phase when a set of XXZ chains are coupled by a weak *purely Ising* interaction when $0 < \Delta < 1$. As the Ising interactions are strengthened, the system will undergo a phase transition into a phase with Néel order on the chains, which is arranged between chains according to the sign of the interaction. In the equivalent language of spinless fermions, the chains are dominantly superconducting and the interchain coupling involves the density alone.

10. SUMMARY

In summary, we have explored quantum frustrated antiferromagnetism on the planar pyrochlore lattice. Despite an enormous classical ($S = \infty$) degeneracy, we find a robust ordering tendency for Heisenberg magnets of any spin, into a valence-bond or a spin solid. For the related problem of stacked square ice (Ising spins), a sliding phase precedes an antiferroelectric ordering transition.

Notes Added. While this paper was under revision, Chakravarty[37] has proposed that the physics of the "d-density wave" state discussed in the cuprate literature[38] can be captured by bond arrow variables that obey the ice rule for a single layer. In this case our analysis of quantum ice and sliding ice has precise correspondences in that problem. Specifically, we predict a high temperature floating phase and low temperature phase with staggered orbital currents selected by quantum fluctuations. Moreover, in

parallel with this work, Starykh *et al.* proposed the existence of a different kind of sliding phase on an *anisotropic* planar pyrochlore lattice, namely one with isotropic Heisenberg exchange and an exchange strength across diagonals which is much stronger than that on the bonds of the underlying square lattice.[39, 40] Further, since this work appeared as a preprint, other groups have studied the $S = 1/2$ Heisenberg magnet on the planar pyrochlore lattice, and found the same bond ordered ground state as us.[41–43]

APPENDIX A. THE QUANTUM DIMER MODEL ON THE PLANAR PYROCHLORE LATTICE

The basis of the Hilbert space is provided by nearest-neighbor dimer coverings of the planar pyrochlore lattice, the corresponding wavefunctions being given by a product wavefunction of spin singlets of the spins on either end of each dimer. One first has to worry about whether this set of states is linearly independent. In this case, this turns out to be a problem as, already for a single tetrahedron, there are three dimer coverings but only two singlet states. For the planar pyrochlore lattice, this can be remedied by restricting the allowed dimer coverings to be those of the underlying square lattice. While this discriminates between horizontal and diagonal bonds of the planar pyrochlore lattice, this does not break any lattice symmetries—unlike in the case of the three-dimensional pyrochlore lattice. For another resolution of this issue, see further down.

The overlap matrix between different dimer coverings, S with matrix elements $S_{pq} = \langle p \,|\, q \rangle$, where $|p\rangle$ labels a dimer covering. After adding a constant $\frac{N_s}{2}\frac{3J}{4}$ to the Hamiltonian (N_s being the number of sites), we compute the Hamiltonian matrix elements H_{pq}, and find that the diagonal terms vanish. The full Hamiltonian matrix for an orthogonalized basis set can be written down as $S^{-1/2}HS^{-1/2}$, as explained in ref. 26, where $S^{-1/2}$ is the matrix square-root inverse of S, obtained by formally carrying out a Taylor expansion in powers of x. Its leading order term at $O(x^0)$ is the unit matrix. In the absence of diagonal terms, the leading order term in H is of $O(x)$. This term is off-diagonal in dimer basis and it effects the resonance move depicted in Eq. (3.1). This is then also the leading order term in $S^{-1/2}HS^{-1/2}$.

The corresponding matrix elements, t_α, depend on whether the resonance loop is around a crossed (t_c) or an uncrossed (t_u) plaquette. One finds $t_c = 0$ and $t_u \neq 0$. The sign of t_u is a matter of convention but it is convenient to choose it to be uniformly positive if possible, as is the case here.

We conclude the appendix by remarking that one could have reached the same result by retaining the diagonal dimers and carrying out the same

formal expansion while disregarding the non-invertibility of S, which would show up in the failure of the series for $S^{-1/2}$ to converge at $x = 1/2$. In that case, the leading order term would still be determined by loops of length four. Since all the loops containing the diagonal dimers either have zero kinetic energy or are longer in length (and thus show up at higher order in x), the resulting quantum dimer model Hamiltonian would be unchanged from Eq. (3.1).

ACKNOWLEDGMENTS

We are grateful to J.-B. Fouet, E. Lieb, S. Palmer, S. Sachdev, S. Shastry, and Ph. Sindzingre for useful discussions, and to C. Henley and C. Lhuillier also for comments on the manuscript. We especially want to thank Ph. Sindzingre for sharing with us his unpublished work on Heisenberg–Ising models, and for a critical reading of the manuscript. We thank P. Chandra for collaboration on related work and P. Schupp for the pyrochlore figure. This work was supported in part by the NSF (Grants DMR-9978074 and DMR-0213706) and the David and Lucile Packard Foundation.

REFERENCES

1. For an introduction to frustrated magnets, see R. Moessner, *Can. J. Phys.* **79**:1283 (2001); reviews of exact diagonalizations and experiments, respectively, are C. Lhuillier, P. Sindzingre, and J.-B. Fouet, *Can. J. Phys.* **79**:1525 (2001) and P. Schiffer and A. P. Ramirez, *Comments Cond. Mat. Phys.* **18**:21 (1996).
2. A. B. Harris, A. J. Berlinsky, and C. Bruder, *J. Appl. Phys.* **69**:5200 (1991).
3. M. Isoda and S. Mori, *J. Phys. Soc. Jpn.* **67**:4022 (1998).
4. B. Canals and C. Lacroix, *Phys. Rev. B* **61**:1149 (2000).
5. A. J. Garcia-Adeva and D. L. Huber, *Phys. Rev. Lett.* **85**:4598 (2000).
6. A. Koga and N. Kawakami, *Phys. Rev. B* **63**:144432 (2001).
7. H. Tsunetsugu, *Phys. Rev. B* **65**:024415 (2002).
8. M. Elhajal, B. Canals, and C. Lacroix, *Can. J. Phys.* **79**:1353 (2001).
9. J. Villain, *Z. Phys. B* **33**:31 (1979).
10. J. N. Reimers, *Phys. Rev. B* **45**:7287 (1992); M. P. Zinkin, M. J. Harris, and T. Zeiske, *Phys. Rev. B* **56**:11786 (1997).
11. R. Moessner and J. T. Chalker, *Phys. Rev. Lett.* **80**:2929 (1998); *Phys. Rev. B* **58**:12049 (1998).
12. The kagome lattice is based on corner-sharing triangles, rather than tetrahedra. Whereas four spins on a single tetrahedron have an internal ground-state degeneracy, three spins on a triangle do not; however, an extensive degeneracy arises as the ground-state constraints of different triangles can cease to be independent, as happens for coplanar states.
13. J. T. Chalker and J. F. G. Eastmond, *Phys. Rev. B* **46**:14201 (1992); P. Lecheminant, B. Bernu, C. Lhuillier, L. Pierre, and P. Sindzingre, *Phys. Rev. B* **56**:2521 (1997).
14. E. H. Lieb, *Phys. Rev. Lett.* **18**:692 (1967).
15. S. E. Palmer and J. T. Chalker, *Phys. Rev. B* **64**:094412 (2001).

16. J.-B. Fouet, M. Mambrini, P. Sindzingre, and C. Lhuillier, *Phys. Rev. B* **67**:054411 (2003).
17. R. R. P. Singh, O. A. Starykh, and P. J. Freitas, *J. Appl. Phys.* **83**:7387 (1998)
18. E. H. Lieb and P. Schupp, *Phys. Rev. Lett.* **83**:5362 (1999).
19. B. Canals and D. Garanin, *Eur. Phys. J. B* **26**:439 (2002)
20. B. Canals, *Phys. Rev. B* **65**:184408 (2002).
21. Ph. Sindzingre, unpublished.
22. C. S. O'Hern, T. C. Lubensky, and J. Toner, *Phys. Rev. Lett.* **83**:2745 (1999); L. Golubovic and M. Golubovic, *Phys. Rev. Lett.* **80**:4341 (1998).
23. D. Arovas and A. Auerbach, *Phys. Rev. Lett.* **61**:617 (1988).
24. S. Sachdev and N. Read, *Int. J. Mod. Phys. B* **5**:219 (1991); N. Read and S. Sachdev, *Phys. Rev. Lett.* **62**:1694 (1989); S. Sachdev, *Phys. Rev. B* **45**:12377 (1992).
25. C. H. Chung, J. B. Marston, and S. Sachdev, *Phys. Rev. B* **64**:134407 (2001).
26. D. S. Rokhsar and S. A. Kivelson, *Phys. Rev. Lett.* **61**:2376 (1988).
27. C. L. Henley and N.-G. Zhang, *Phys. Rev. Lett.* **81**:5221 (1998); C. L. Henley, *Can. J. Phys.* **79**:1307 (2001) and forthcoming publication.
28. O. Tchernyshyov, O. A. Starykh, R. Moessner, and A. G. Abanov, *Phys. Rev. B* **68**:144422 (2003).
29. O. Tchernyshyov *et al.*, work in progress.
30. Also, these authors point out that several of the smaller systems display symmetries on top of the ones present for the infinite lattice.
31. R. Moessner, S. L. Sondhi, and P. Chandra, *Phys. Rev. Lett.* **84**:4457 (2000); R. Moessner and S. L. Sondhi, *Phys. Rev. B* **63**:224401 (2001).
32. P. W. Anderson, *Phys. Rev.* **102**:1008 (1956).
33. For an introduction to height representation theory close to the perspective of this paper, see C. Zeng and C. L. Henley, *Phys. Rev. B* **55**:14935 (1997).
34. R. Youngblood, J. D. Axe, and B. M. McCoy, *Phys. Rev. B* **21**:5212 (1980).
35. S. Lukyanov, *Phys. Rev. B* **59**:11163 (1999). The derivation is given in S. Lukyanov and V. Terras, hep-th/0206093.
36. The correlations in this phase are governed by the Gaussian combination of Eqs. (8.5) and (8.6). These lead to a factorized height correlator whose in plane form is different from that for an uncoupled plane only by an overall normalization. That in turn, is small at small interlayer coupling.
37. S. Chakravarty, *Phys. Rev. B* **66**:224505 (2002).
38. S. Chakravarty, R. B. Laughlin, D. K. Morr, and C. Nayak, *Phys. Rev. B* **63**:094503 (2001).
39. O. A. Starykh, R. R. P. Singh, and G. C. Levine, *Phys. Rev. Lett.* **88**:167203 (2002).
40. P. Sindzingre, J.-B. Fouet, and C. Lhuillier, *Phys. Rev. B* **66**:174424 (2002).
41. W. Brenig and A. Honecker, *Phys. Rev. B* **65**:140407 (2002).
42. B. Canals, *Phys. Rev. B* **65**:184408 (2002).
43. E. Berg, E. Altman, and A. Auerbach, *Phys. Rev. Lett.* **90**:147204 (2003).